AD-A018 900

LASER ABSORPTION STUDIES

F. S. Mills, et al

Ohio State University

Prepared for:

Rome Air Development Center
Defense Advanced Research Projects Agency

November 1975

RADC-TR-75-289
Interim Report
November 1975

LASER ABSORPTION STUDIES

Ohio State University

Sponsored by
Defense Advanced Research Projects Agency
ARPA Order No. 1279

Approved for public release;
distribution unlimited.

The views and conclusions contained in this document are those of the authors and should not be interpreted as necessarily representing the official policies, either expressed or implied, of the Defense Advanced Research Projects Agency or the U. S. Government.

Rome Air Development Center
Air Force Systems Command
Griffiss Air Force Base, New York 13441

UNCLASSIFIED

SECURITY CLASSIFICATION OF THIS PAGE (When Data Entered)

REPORT DOCUMENTATION PAGE		READ INSTRUCTIONS BEFORE COMPLETING FORM
1. REPORT NUMBER RADC-TR-75-289	2. GOVT ACCESSION NO.	3. RECIPIENT'S CATALOG NUMBER
4. TITLE (and Subtitle) LASER ABSORPTION STUDIES		5. TYPE OF REPORT & PERIOD COVERED 1st Interim Report 1 Oct 74 - 1 Apr 75
		6. PERFORMING ORG. REPORT NUMBER ESL 4054-2
7. AUTHOR(s) F. S. Mills R. K. Long E. K. Damon		8. CONTRACT OR GRANT NUMBER(s) F30602-75-C-0029
9. PERFORMING ORGANIZATION NAME AND ADDRESS Ohio State University ElectroScience Laboratory Department of Electrical Engineering Columbus OH 43212		10. PROGRAM ELEMENT, PROJECT, TASK AREA & WORK UNIT NUMBERS 62301E 12790506
11. CONTROLLING OFFICE NAME AND ADDRESS Defense Advanced Research Projects Agency 1400 Wilson Blvd Arlington VA 22209		12. REPORT DATE November 1975 13. NUMBER OF PAGES 40
14. MONITORING AGENCY NAME & ADDRESS(if different from Controlling Office) Rome Air Development Center (OCSE) Griffiss AFB NY 13441		15. SECURITY CLASS. (of this report) UNCLASSIFIED 15a. DECLASSIFICATION/DOWNGRADING SCHEDULE N/A

16. DISTRIBUTION STATEMENT (of this Report)

Approved for public release; distribution unlimited.

17. DISTRIBUTION STATEMENT (of the abstract entered in Block 20, if different from Report)

Same

18. SUPPLEMENTARY NOTES

RADC Project Engineer:
James W. Cusack/OCSE

19. KEY WORDS (Continue on reverse side if necessary and identify by block number)

molecular absorption laser
laser
laser propagation
DF laser

20. ABSTRACT (Continue on reverse side if necessary and identify by block number)

This report covers progress on the various tasks which comprise the subject research program. These tasks include DF laser measurements for HD_0 and H_20 absorbers and CO_2 laser absorption measurements on the P(20) and R (20) lines. Additional topics include spectrophone calibration techniques, improvements in calculation programs and design of CO, CO_2 and DF probe lasers.

DD FORM 1 JAN 73 1473 EDITION OF 1 NOV 65 IS OBSOLETE

UNCLASSIFIED

SECURITY CLASSIFICATION OF THIS PAGE (When Data Entered)

LASER ABSORPTION STUDIES

F. S. Mills
R. K. Long
E. K. Damon

Contractor: The Ohio State University
Contract Number: F30602-75-C-0029
Effective Date of Contract: 1 October 1974
Contract Expiration Date: 30 September 1975
Amount of Contract: $124,969.00
Program Code Number: 5E20
Period of work covered: 1 Oct 74 - 1 Apr 75

Principal Investigator: Dr. Ronald K. Long
Phone: 614 422-6077

Project Engineer: James W. Cusack
Phone: 315 330-3145

This research was supported by the Defense Advanced Research Projects Agency of the Department of Defense and was monitored by James W. Cusack, RADC (OCSE), Griffiss Air Force Base, New York 13441.

This report has been reviewed by the RADC Information Office (OI) and is releasable to the National Technical Information Service (NTIS). At NTIS it will be releasable to the general public including foreign nations.

This technical report has been reviewed and is approved for publication.

APPROVED: James W Cusack

JAMES W. CUSACK
Project Engineer

Do not return this copy. Retain or destroy.

TABLE OF CONTENTS

		Page
I.	HDO MEASUREMENTS ON 2-1 P(6), P(7), AND P(8) DF LINES	1
II.	H_2O ABSORPTION MEASUREMENTS ON 2-1 P(6), P(7), AND P(8)	5
III.	WHITE CELL IMPROVEMENTS	9
IV.	SMALL PULSED DF LASER	11
V.	IMPROVEMENTS IN CALCULATION PROGRAMS	14
VI.	CO_2 LASER MEASUREMENTS	19
	A. Background	19
	B. Measurements on P(20) Line	19
	C. Measurements on R20 Line	23
VII.	SPECTROPHONE CALIBRATION TECHNIQUES	27
VIII.	DIODE LASER SPECTROSCOPY	31
IX.	DESIGN OF CO, CO_2, AND DF PROBE LASERS	32
REFERENCES		33

I. HDO MEASUREMENTS ON 2-1 P(6), P(7), AND P(8) DF LINES

Absorption of the 2-1 P(6), P(7), and P(8) DF laser lines by HDO-nitrogen mixtures has been measured. An earlier report gave results for the 3-2 P(6), P(7), and P(8) lines [2]. The equipment, data recording procedures, and sample preparation techniques have been described in earlier reports [1, 2] and will therefore not be repeated here.

The lead selenide detectors were recalibrated for linearity prior to these measurements. This was necessary since some time had elapsed since the last calibration and the last calibration had been done for the 3-2 DF lines which have a lower power level than the 2-1 lines. The calibration procedure was the same as described earlier [1].

The water samples used were: for the 2-1 P(6) line, .01% D_2O, 1.99% HDO, balance H_2O; for the 2-1 P(7) line, .003% D_2O, 1.02% HDO, balance H_2O; and for the 2-1 P(8) line, .12% D_2O, 6.22% HDO, balance H_2O. The mixtures were chosen so that the absorption could be accurately measured in a 731.7 meter path.

Figures 1, 2, and 3 show the results for the 2-1 P(6), P(7), and P(8) lines, respectively. The absorption cell path length was 731.7 meters, and it originally contained 15 torr of the HDO-enriched water mixture plus nitrogen to a total pressure of 760 torr. The lower points on the curve were then obtained by partially pumping out the sample and refilling with nitrogen to 760 torr.

For each line a least squares fit of the data to an expression of the form $k = Ap + Bp^2$ was made, where k is the absorption coefficient and p is the partial pressure of enriched water vapor in torr. The derived expression is presumed to be a more accurate characterization of the absorption coefficient than any individual data point. For the 2-1 P(6) line, the derived expression is:

$$k = .225\ p + 1.36 \times 10^{-3}\ p^2\ km^{-1};$$

for 2-1 P(7),

$$k = .202\ p + 1.78 \times 10^{-3}\ p^2\ km^{-1};$$

and for 2-1 P(8),

$$k = 7.00 \times 10^{-2}\ p + 1.20 \times 10^{-3}\ p^2\ km^{-1},$$

with p in torr.

In Table I the above expressions are listed as extrapolated to an assumed abundance of HDO and H_2O of 0.03% along with the expressions obtained previously for the 3-2 lines. This was done by multiplying the coefficients A and B by .03/x, where x is the percent HDO concentration of the mixture used to make the measurements.

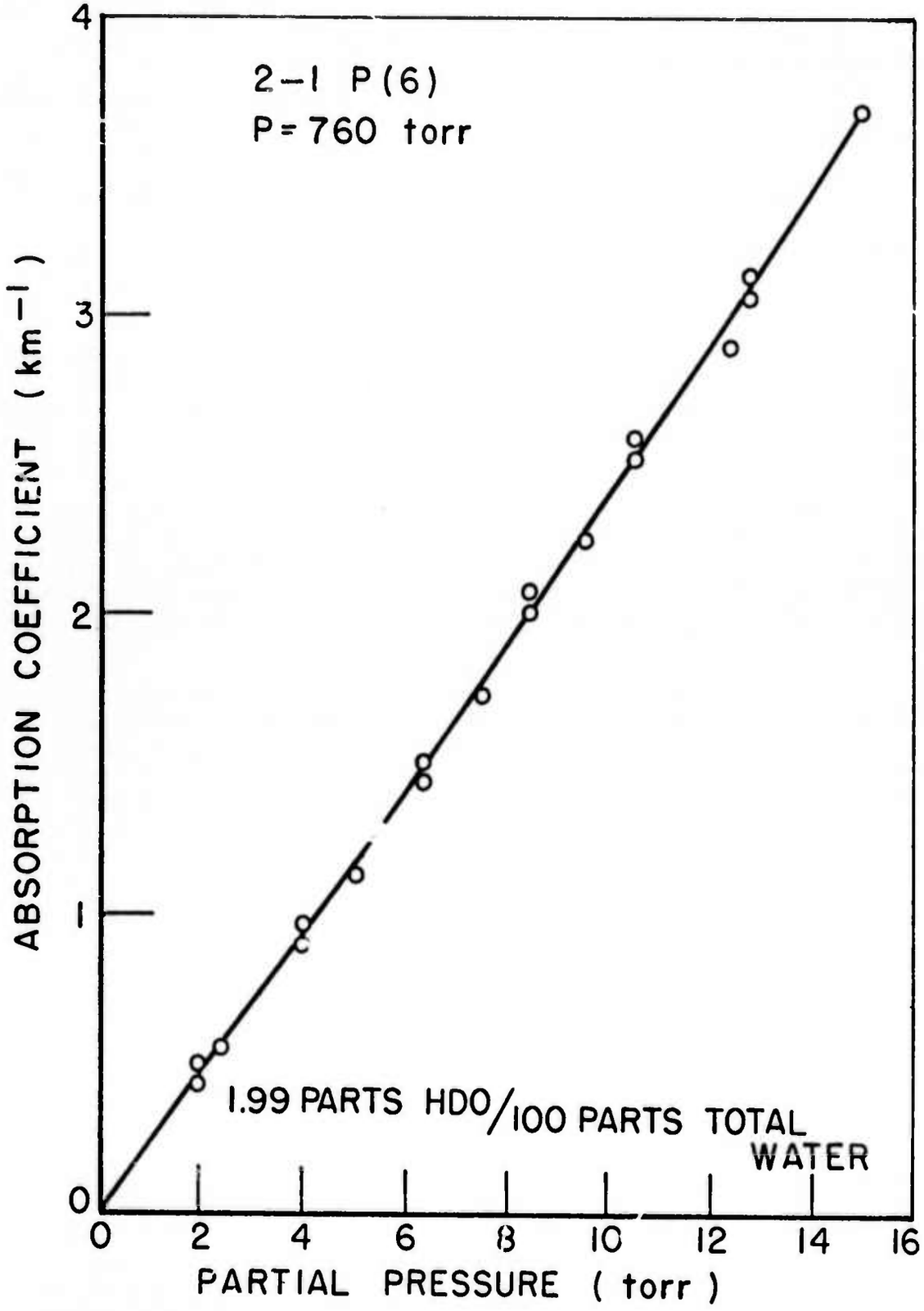

Fig. 1. HDO absorption for the 2-1 P(6) DF laser line.

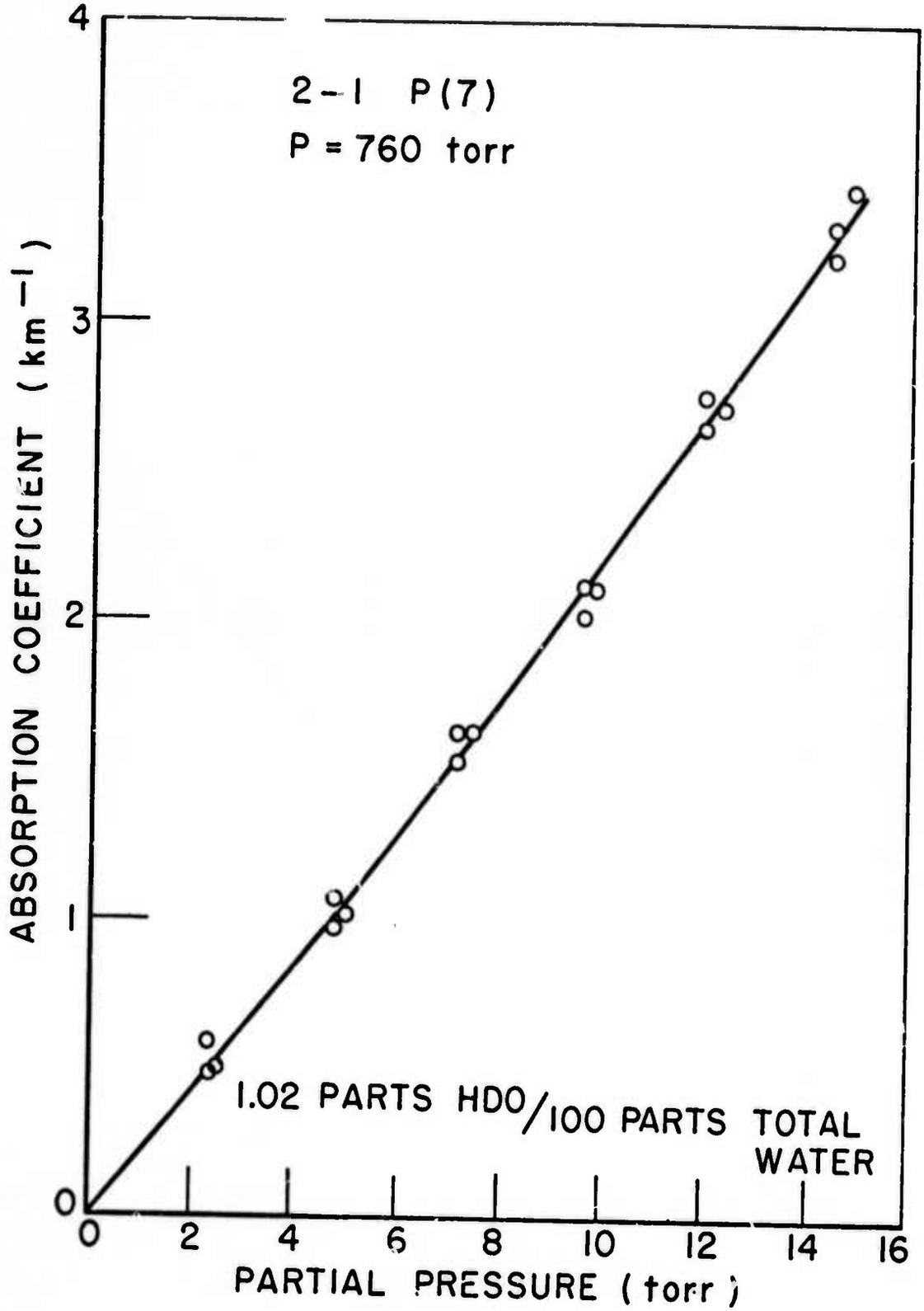

Fig. 2. HDO absorption for the 2-1 P(7) DF laser line.

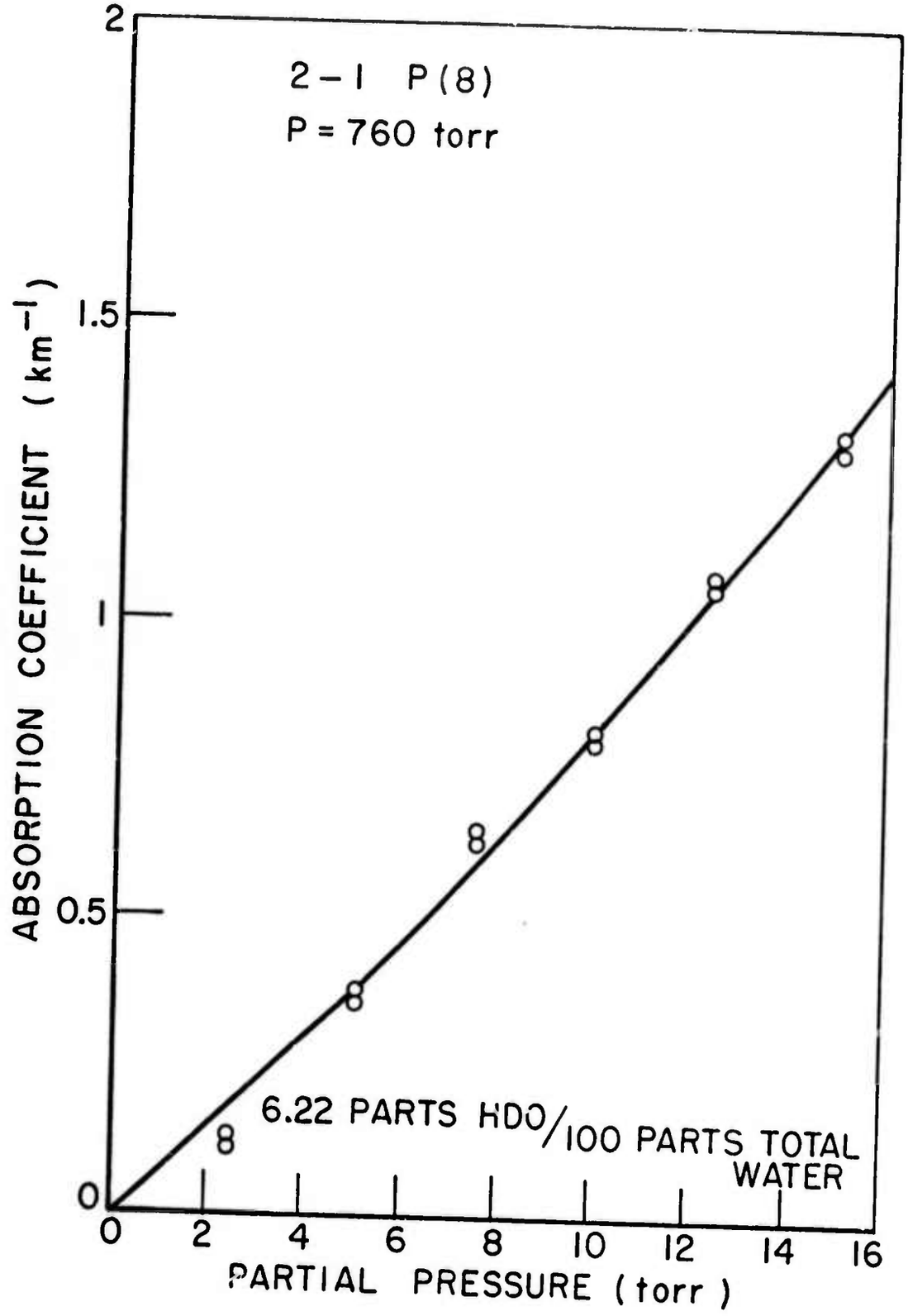

Fig. 3. HDO absorption for the 2-1 P(8) DF laser line.

These expressions have been evaluated at 14.26 torr for each line and the values listed in Table I along with the absorption coefficients predicted from the AFCRL tape.

It should be pointed out that the expressions for absorption coefficients in Table I are only valid at 24°C and 760 torr total pressure. The temperature dependence and total pressure dependence of tne absorption coefficients nave not been investigated experimentally.

TABLE I

Ident	ν (cm^{-1})	K_{exp} .03% HDO, 760 Torr Total pressure (Km^{-1})	K_{exp} 14.26 Torr H_2O (Km^{-1})	$K_{calc.}$ 14.26 Torr H_2O (Km^{-1})
2-1 P(6)	2680.178	$3.39 \times 10^{-3}\ p + 2.05 \times 10^{-5}\ p^2$	5.24×10^{-2}	3.71×10^{-2}
2-1 P(7)	2655.863	$5.94 \times 10^{-3}\ p + 5.24 \times 10^{-5}\ p^2$	9.54×10^{-2}	7.25×10^{-2}
2-1 P(8)	2631.067	$3.38 \times 10^{-4}\ p + 5.78 \times 10^{-6}\ p^2$	6.00×10^{-3}	9.14×10^{-3}
3-2 P(6)	2594.198	$1.11 \times 10^{-3}\ p + 7.62 \times 10^{-6}\ p^2$	1.74×10^{-2}	7.23×10^{-3}
3-2 P(7)	2570.522	$4.71 \times 10^{-4}\ p + 9.31 \times 10^{-6}\ p^2$	5.61×10^{-3}	4.63×10^{-3}
3-2 P(8)	2546.375	$1.45 \times 10^{-4}\ p + 1.93 \times 10^{-6}\ p^2$	2.46×10^{-3}	1.15×10^{-3}

Since the water samples used also contained an enhanced D_2O concentration as well as enhanced HDO, it is possible tnat some error might be introduced due to the D_2O absorption. This possibility was investigated at each of the 2-1 lines by measuring the absorption of a sample of pure D_2O vapor broadened with dry air. Tne D_2O vapor pressure was 0.21 torr which is 12-500 times the D_2O partial pressures at the highest water vapor pressure for the HDO measurements presented in Figures 1, 2, and 3. There was measurable D_2O absorption, however if the measurements are extrapolated to the conditions prevailing in the HDO absorption measurements the D_2O contribution to the absorption coefficient at the highest water vapor pressure is .02 or .03 which is less than the scatter in the experimental data. Therefore, D_2O absorption may be safely ruled out as a source of error in the HDO absorption measurements for the 2-1 laser lines.

II. H_2O ABSORPTION MEASUREMENTS ON 2-1 P(6), P(7), AND P(8)

Absorption of the 2-1 P(6), P(7), and P(8) DF laser lines by H_2O-air and H_2O-nitrogen mixtures has been measured. It was originally thought that water absorption would be too small to measure accurately in the White cell at room temperature. However, preliminary spectrophone measurements made at United Aircraft Corporation [4] indicated higher absorption on some lines than had been expected. It was therefore decided that with a very carefully performed experiment it might be possible to measure the absorption directly in the White cell.

Improvements in the White cell optics which are discussed later in this report made it possible to increase the path length to 1.34 kilometers with only a small increase in insertion loss. Also, a new pulsed laser was constructed which was primarily intended to eliminate RF noise emission. While testing the new laser, it was also found that the average power was improved significantly over the earlier model. This made possible the use of thermopile detectors which eliminated the need for detector linearity correction which had been a source of error with the measurements using the lead selenide detectors.

The thermopiles were carefully shielded in styrofoam to reduce the effect of air currents and short term fluctuations in room temperature.

In previous measurements the ratio of input to output for the evacuated cell and the cell filled with the desired sample has been determined by making 500 separate measurements of the ratio over about a 1 minute period and using the average as the final value. The sample transmittance is then just the quotient of the ratio obtained with the sample in the cell and the ratio obtained with the cell evaluated. The absorption coefficient is then obtained by dividing the negative of the natural logarithm of the transmittance by the path length.

For the measurements of HDO, H_2O, and CH_4 absorption it was possible to measure the absorption coefficient at several absorber concentrations and use least-squares curve-fitting techniques to improve the accuracy of the measurements. This was not possible for the H_2O measurements, however, since the absorption at the highest water vapor pressure was still quite low.

The procedure used therefore was to repeat the measurement of input to output ratio described above several times in a period of a half-hour. These ratios are then averaged to obtain a final value. Also, the ratio for the evacuated cell is measured both before and after the measurement of ratio for the sample. Transmittances may then be calculated using each empty cell ratio separately or the average of the ratios. The entire procedure was repeated two or three times for each line, i.e., on different days and different water samples.

Measurements were made with a path length of 1.341 km., water vapor pressure of 14.3 torr and total pressure including dry air or nitrogen of 760 torr. Both dry air and nitrogen were used as broadening gases, and within error limits no difference in absorption coefficient was observed. Also, there was no observable difference between the transmittance of the evacuated cell and the transmittance of the cell when filled with either dry air or nitrogen.

The data are presented in Tables II, III, and IV for the 2-1 P(6), P(7), and P(8) DF laser lines. The ratio of input to output measured with the sample in the cell is designated R_i. The ratio measured for the evacuated cell before the sample is admitted is BK_{i1}, and the ratio measured when the cell is evacuated after measuring the sample is designated BK_{i2}.

TABLE II

H_2O ABSORPTION ON THE 2-1 P(6) DF LASER LINE AT 2680.178 cm^{-1}

	T	K (km^{-1})	Avg K (km^{-1})
R1/BK11 = 1.071/1.183	0.905	0.074	
R1/BK12 = 1.071/1/182	0.906	0.074	0.075
R2/BK21 = 1.071/1.181	0.097	0.073	
R2/BK22 = 1.071/1.192	0.898	0.080	
$R1/\frac{BK11+BK12}{2}$ = 1.071/1.1825	0.906	0.074	
$R2/\frac{BK21+BK22}{2}$ = 1.071/1.1865	0.903	0.076	0.075

TABLE III

H_2O ABSORPTION ON THE 2-1 P(7) DF LASER LINE AT 2655.863 cm^{-1}

	T	K (km^{-1})	Avg K (km^{-1})
R1/BK11 = 1.055/1.196	0.882	0.094	
R1/BK12 = 1.055/1.204	0.876	0.099	
R2/BK21 = 1.033/1.204	0.858	0.114	0.103
R2/BK22 = 1.033/1.211	0.853	0.119	
R3/BK31 = 1.045/1.211	0.863	0.110	
R3/BK32 = 1.045/1.170	0.893	0.084	
$R1/\frac{BK11+BK12}{2}$ = 1.055/1.200	0.879	0.096	
$R2/\frac{BK21+BK22}{2}$ = 1.033/1.208	0.855	0.116	0.103
$R3/\frac{BK31+BK32}{2}$ = 1.045/1.191	0.878	0.097	

TABLE IV

H_2O ABSORPTION ON THE 2-1 P(8) DF LASER LINE AT 2631.067 cm^{-1}

	T	K (km^{-1})	Avg K (km^{-1})
R1/BK11 = 1.422/1.499	0.948	0.039	
R1/BK12 = 1.422/1.484	0.958	0.032	
R2/BK21 = 1.414/1.484	0.953	0.036	0.0375
R2/BK22 = 1.414/1.498	0.944	0.043	
$R2/\frac{BK11+BK12}{2}$ = 1.422/1.492	0.953	0.036	
$R2/\frac{BK21+BK22}{2}$ = 1.414/1.491	0.948	0.040	0.038

In Table V the average values for each line are compared with the HDO measurements reported earlier in this report; calculated H_2O values from the AFCRL tape; and H_2O continuum values obtained using Burch's data [22].

TABLE V

Line	1 H_2O calc (km^{-1})	2 HDO measured (km^{-1})	3 Burch continuum (km^{-1})	1+2+3 (km^{-1})	H_2O measured (km^{-1})
2-1 P(6)	2.44×10^{-4}	5.24×10^{-2}	2.12×10^{-2}	7.38×10^{-2}	7.5×10^{-2}
2-1 P(7)	4.61×10^{-6}	9.54×10^{-2}	1.93×10^{-2}	1.15×10^{-1}	1.03×10^{-1}
2-1 P(8)	5.05×10^{-3}	6.00×10^{-3}	1.78×10^{-2}	2.89×10^{-2}	3.8×10^{-2}

On the 2-1 P(6) line, calculated H_2O is very small and the measured HDO absorption plus Burch continuum agree quite well with the measured H_2O value. Agreement is not as good on the 2-1 P(7) line, although the HDO measurement added to the continuum value is certainly within the experimental scatter shown in Table III. On the 2-1 P(8) line, agreement is again only fair although here the difference could be attributed to an error in calculating the local water contribution.

In conclusion, it would appear from these measurements that the continuum calculated by extrapolating Burch's high temperature measurements is very nearly correct.

III. WHITE CELL IMPROVEMENTS

Improvements have been made in the White cell which helped make the H_2O measurements just described possible.

First, the White cell mirrors were cleaned using a mild detergent and rinsed with distilled water and ethanol. This increased the mirror reflectivity and reduced the insertion loss.

When an attempt was made to increase the path length from .732 to 1.341 kilometers (48 to 88 traversals), it was discovered that the output spot size had increased so much that the spots overlapped on the single mirror. Using a program which calculated the spot size of a Gaussian laser beam anywhere in an optical system containing up to 10 elements, it was discovered that error in mirror separation in the White cell would cause the spot at the single mirror to grow as the path length was increased. That is, the White cell mirrors must be separated by exactly their radius of curvature. There is some small increase in spot size if the beam is not focussed properly at the entrance to the White cell, but the increase is small and it is not cumulative.

The mirror separation was adjusted using a white light source and the optical setup shown in Fig. 4. An image was formed at point O in the plane of mirror C which then filled mirror A. The image was observed in the plane of mirror C at the output with the cell set for 64 passes. The separation was then adjusted to make that image as sharp as possible.

It was found that the mirrors had been about 1 cm too far apart. Since the mirror separation is 15.24 meters, this is not a large error, but it does cause problems if long path lengths are desired. The 1 cm error did not cause a problem with the White cell set at .7317 km.

From the above discussion, it is obvious that for a White cell which is designed to be either heated or cooled some provision must be made for keeping the mirrors properly separated as the cell expands and contracts.

With the above improvements, it was possible to use the White cell at 88 traversals. With the large number of traversals a very small change in the position of mirror A or B causes a noticeable movement in the position of the output spot. It is therefore necessary to monitor the position of the output spot and the number of traversals before each measurement and readjust the spot position if there has been a change.

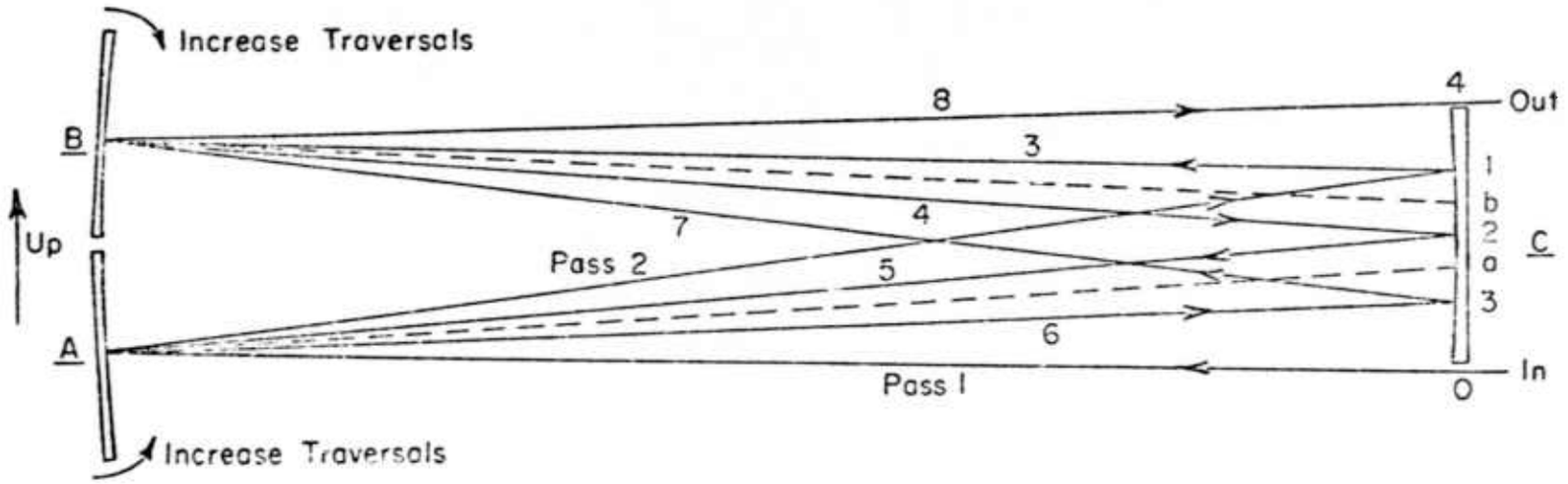

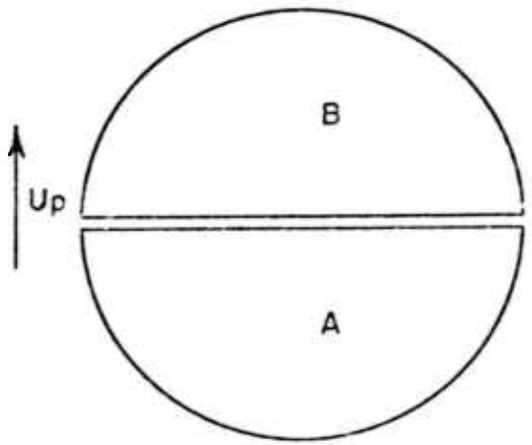

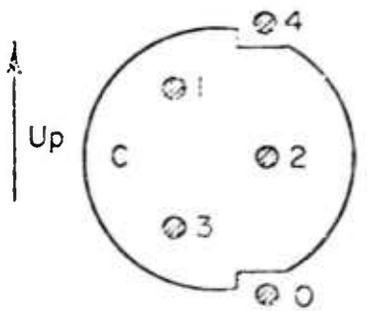

Fig. 4. Ray diagram of White cell.

IV. SMALL PULSED DF LASER

Although the pulsed laser used previously was fairly satisfactory, it was decided that a more portable laser was needed. In particular, a laser was needed which had very little RF noise emission, since the large shielded room was taking up much needed laboratory space. It was also felt that improved optical stability could be maintained if the laser could be mounted on the same table with the White cell entrance optics.

The previous laser used a high voltage power supply to charge a capacitor to 12-15 kv. The capacitor was then discharged through a thyratron to excite the laser. This arrangement caused a great deal of RF noise emission.

The small pulsed laser built by Ultee [5] used a different power supply design than that described above. Ultee's power supply charged a 1 microfarad capacitor to about 600 volts and discharged it through a pulse transformer to get the high voltage required by the laser tube. This design has the advantage that the high-voltage pulses are restricted to the output of the pulse transformer and the laser tube. These components can be fairly easily shielded to eliminate RF noise emission. Using circuit diagrams provided by Ultee, a pulser has been constructed.

Also, a new tube has been designed and built which has an active length of 20 centimeters and inside diameter of 5.5 millimeters. This compares to an active length of about 30 centimeters and inside diameter of 8.7 millimeters for the previous laser. The new tube has one inlet at the center of the tube for the main gas mixture, and an exhaust port at either end as well as helium inlet ports at the Brewster windows.

It had been observed on the previous laser that the copper electrodes became fouled after a period of time, particularly the one at the high-voltage end. This could possibly have been copper sulfate. A couple of different electrode configurations were tried. The most satisfactory solution seems to be a nickel rod at the low-voltage end, and a tungsten rod at the high-voltage end insulated with teflon tape except at the tip.

The optical cavity for the new laser consists of a 300 line/mm grating blazed at 3.5μm and a 20 meter radius of curvature Germanium mirror coated for greater than 80% reflectivity between 3μm and 4μm. The grating and mirror are separated by 80 cm. The grating mount is of the same design as that used on the previous laser. The output mirror is mounted in a commercial gimbal mount.

The laser is constructed on a 3/4" aluminum plate, ten inches wide and thirty-nine inches long. Along one side of the laser is a 1/4" aluminum plate. Attached to the plate are a box containing the oscillator, feedthroughs for the gases and a vacuum gauge which reads the pressure at

the exhaust ports of the laser tube. The mirror mount, grating mount, laser tube, storage capacitor, thyratron, and pulse transformer are all mounted on the base plate. There is an aluminum box attached to the base plate and side plate which encloses everything but the mirror mount and grating mount. There are small holes in the ends of the box to let the laser beam out. Figure 5 shows the laser with the shield box removed.

Since the laser tube was not exactly the same as Ultee's, it was necessary to use a different pulse transformer and storage capacitor. The DC voltage to charge the capacitor is supplied by a photomultiplier tube supply. The capacitor is charged to about 1200 to 1300 volts.

The new laser completely eliminated the RF noise emission experienced with the earlier laser and in addition the average power is increased by a factor of four or five. Part of the increase comes from a faster pulse rate (50 pps rather than 35) made possible because the tube is smaller and the vacuum pump is the same (500 l/m).

A second laser very similar to the one described above was built and loaned to Professor Rao in the Ohio State University Physics Department so the laser line frequencies could be measured using a very accurate grating spectrometer. The values are given in Table VI for each of the lines observed in the small laser. The accuracy of the measurements is ± .003 cm.

An accurate knowledge of the line frequencies is necessary in order to make more accurate predictions of the absorption coefficients using the AFCRL line data.

TABLE VI

OBSERVED DF LASER LINES

Identification Band	Transition	Frequency (cm-1)	Identification Band	Transition	Frequency (cm-1)	Identification Band	Transition	Frequency (cm-1)
*1-0	P(2)	2862.653	2-1	P(2)	2772.340	*3-2	P(2)	2683.890
1-0	P(3)	2839.791	2-1	P(3)	2750.094	3-2	P(3)	2662.246
1-0	P(4)	2816.380	2-1	P(4)	2727.309	3-2	P(4)	2640.074
1-0	P(5)	2792.434	2-1	P(5)	2703.999	3-2	P(5)	2617.386
1-0	P(6)	2767.968	2-1	P(6)	2680.179	3-2	P(6)	2594.198
1-0	P(7)	2742.998	2-1	P(7)	2655.863	3-2	P(7)	2570.522
1-0	P(8)	2717.539	2-1	P(8)	2631.068	3-2	P(8)	2546.375
1-0	P(9)	2691.607	2-1	P(9)	2605.807	3-2	P(9)	2521.769
1-0	P(10)	2665.219	2-1	P(10)	2580.097	3-2	P(10)	2496.721
1-0	P(11)	2638.392	2-1	P(11)	2553.953	3-2	P(11)	2471.245
*1-0	P(12)	2611.142	2-1	P(12)	2527.391	*3-2	P(12)	2445.356
*1-0	P(13)	2583.486	*2-1	P(13)	2500.428	*3-2	P(13)	2419.070

* Not observed in this laser, included for convenience.

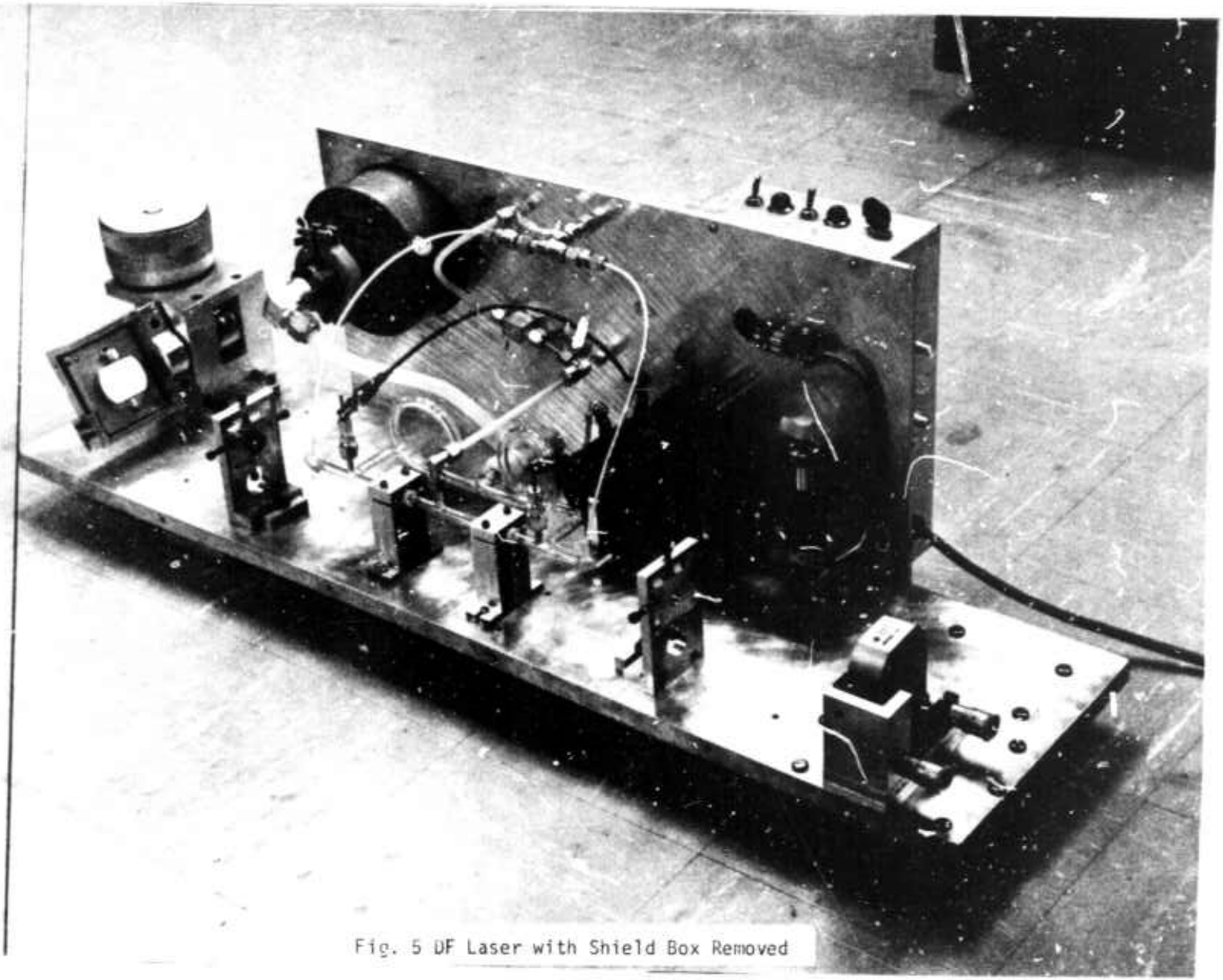

Fig. 5 DF Laser with Shield Box Removed

V. IMPROVEMENTS IN CALCULATION PROGRAMS

Calculations made from the AFCRL Line Compilation tape are a very useful guide to the experimental work. Past experience has shown that the calculations are frequently in error quantitatively by a factor of 2 or more. However, they are generally good qualitatively and give a reasonably accurate picture of the character of the absorption spectrum near a laser frequency of interest provided all the pertinent absorption lines are listed.

There are basically two programs used. One calculates synthetic spectra and the other calculates single frequency absorption. The programs have been described before [6, 7], however, since modifications have since been made, the descriptions will be repeated here including the modifications.

The most recent modifications are (1) the addition of the Voigt profile to both programs so that calculations may be made at low pressures and (2) the output of the plot program has been changed so that the absorption coefficient rather than the transmittance is plotted.

The basic quantity calculated by the programs is

$$(1) \qquad -\ln(\text{transmittance}) = k'u$$

where k' is in units $(\text{mol} - \text{cm}^{-2})^{-1}$ and u is in units $\text{mol}-\text{cm}^{-2}$. There are two different equations used to calculate k' depending on the total pressure. For pressures above about 75 torr, the Lorentz profile is used:

$$(2) \qquad k' = \frac{S}{\pi} \frac{\alpha_L}{(\nu - \nu_0)^2 + \alpha_L^2}$$

For lower pressures, the Voigt profile is used:

$$(3) \qquad k' = \frac{S\alpha_L}{\pi^{3/2}} \int_{-\infty}^{\infty} \frac{e^{-t^2} \, dt}{\alpha_L^2 + \left[\nu - \nu_0 - \frac{\alpha_D t}{(\ell n 2)^{1/2}}\right]^2}$$

In the above equations, S is the line strength; α_D, the Doppler half-width, is given by

$$(4) \qquad \alpha_D = 3.5812 \times 10^{-7} \left(\frac{T}{M}\right)^{1/2} \nu_0$$

where T is the temperature in degrees k, M is the molecular weights of the molecule, and ν_0 is the transition frequency.

The Lorentz half-width at standard temperature and pressure is read from the data tape. This value must then be corrected for the conditions of pressure and temperature of the model atmosphere.

In order to derive the required relationships, it is useful to write the kinetic theory half-width as follows:

$$(5) \qquad \alpha_L = \left(\frac{1}{8\pi kT}\right)^{1/2} C_{aN_2} \, Pe$$

where k is Boltzmann's constant, CaN_2 is a constant related to the sum of the optical collision diameters and the mass of the absorbing molecule and nitrogen, and Pe is the effective pressure given in general by

$$(6) \qquad Pe = Pa\ B + \sum_i P_i \, F_i$$

Here Pa is the partial pressure of the absorbing gas, B is the self-broadening gas i. Note that F for nitrogen is defined to be one.

For each absorption line, the AFCRL line compilation gives the line frequency in cm^{-1}, the line strength in $cm^{-1} - (mol - cm^{-2})^{-1}$ at 296 K, the Lorentz half-width in $cm^{-1} - atm^{-1}$ at 296 K, the energy of the lower energy state of the transition in cm^{-1}, the energy levels involved in the transition, and the isotope and type of molecule. For use at temperatures other than 296 K and pressures different from one atmosphere, the line strength and half-width must be corrected using the following equations:

$$(7) \qquad S = S \, \frac{Q_{vo}}{Q_v} \left(\frac{To}{T}\right)^{BX} e^{\frac{E^e}{k}\left(\frac{T - To}{T\,T_o}\right)}$$

and

$$(8) \qquad \alpha_L = \alpha_{Lo} \left(\frac{Pe}{Po}\right)\left(\frac{To}{T}\right)^{CX}$$

where subscript o refers to the values given in the compilation, Qv is the vibrational partition function, $(To/T)^{BX}$ is the ratio of the rotational partition functions, and E^e is the energy of the lower energy state.

Equation 8 follows from equation (5). The exponent on $\frac{To}{T}$ is given as CX rather than 1/2 since it has been determined experimentally that CX is actually about .58 for CO_2 and .62 for H_2O [9, 14].

The vibrational partition functions have been given by McClatchey [8]. At OSU, however, the ratio of vibrational partition functions Q_{VO}/Q_V has been taken to be nearly one and therefore ignored although it could be included if uncertainties in line-shape and half-width were reduced to the point where errors in Q_{VO}/Q_V were significant.

Assuming 296°K for To, 1 atm for Po and using k = .6951 $cm^{-1}/°K$, the strength and half-width corrections become

$$S = S_o \left(\frac{296}{T}\right)^{BX} e^{\frac{E_\ell}{.6951}\left(\frac{T-296}{296T}\right)} \tag{9}$$

and

$$\alpha_L = \alpha_{Lo} P_e \left(\frac{T_o}{296}\right)^{CX} \tag{10}$$

The assumed values for the self-broadening coefficient B, BX, and CX are given for each molecule in Table VII.

TABLE VII

Molecule	B	BX	CX
N_2O	1.24	1.0	.5
CH_4	1.3	1.5	.5
H_2O	5.0	1.5	.62
CO_2	1.3	1.0	.58
O_3	1.0	1.5	.5
CO	1.02	1.0	.5

Equation (2) gives the absorption coefficient k' for one absorption line. At any frequency there might be several lines contributing to the absorption. In that case, k' would be given by the summation of all the individual line contributions, i.e.

$$(11) \qquad k' = \frac{1}{\pi} \sum_i \frac{S_i \alpha_{ii}}{(\nu - \nu_i)^2 + \alpha_{ii}^2}$$

The first program to be described calculates and plots k in km^{-1} versus wavenumber. Note that k in km^{-1} is just k'u, where u is evaluated using the following equation with the path length, L, being one kilometer,

$$(12) \qquad u\ (\text{molecules/cm}^2) = 2.69 \times 10^{19}\ p\ (\text{atm})\ L\ (\text{cm})\ (273/T).$$

Input parameters are the number of absorbers to be considered; the number of plots to be made; the beginning wavenumber of the first plot; the number of wavenumbers per plot; the total pressure in torr; the temperature; the molecule ID number, desired isotope, partial pressure in torr, and broadening coefficient for each absorber type; and descriptive information which is to be written on the plots. The user may specify a continuum of the form $k_c(\nu) = A_0 + A_1\nu + A_2\nu^2$ which is added to the calculated $k(\nu)$ at each point on the plot. The user may also specify a set of frequencies corresponding to laser lines or just frequencies of interest, and the program draws a vertical line on the plot at each specified frequency. The program then calculates u for each absorber from the partial pressure and temperature using Equation (12) and P_e for each absorber from the partial pressure, total pressure, and self-broadening coefficient. Data are read from the AFCRL tape as required and the strength and half-width are corrected for temperature and pressure using Equations (9) and (10). There is a parameter SLOW in the program which may be set to ignore all lines with strength less than SLOW and thus speed the calculation.

The heart of the program is the subroutine which calculates k'u. It is adapted from one written by Deutschman and Calfee [9]. At any point ν, the subroutine considers contributions from absorption lines within BOUND of ν in either direction. Recognizing the uncertainty in the Lorentz line shape at frequencies far from line center, BOUND is usually set to 20 or 25 cm^{-1}. For each separate absorption line in the range $\nu \pm$ BOUND, the subroutine calculates the contribution using either Equation (2) (Lorentz profile) or Equation (3) (Voigt profile), and the appropriate u for the absorber being considered. Whether the Lorentz or Voigt profile is used is determined by the ratio α_L/α_D is greater

than five the Lorentz profile is used, otherwise the Voigt profile is used. The contributions from each absorption line are then added togetner to get the total k'u for local line absorption. If the user has specified a continuum, it is evaluated at this time at the frequency ν and added to k'u. This procedure is repeated for each point on the plot.

The program plots the absorption coefficient in km^{-1} on a logarithmic scale with the scale limits calculated automatically for the most effective presentation.

Earlier versions of this program plotted the transmittance rather than the absorption coefficient. It would seem, however, that this is less desirable since by improper choice of path length and absorber amount it would be possible to calculate a spectrum showing total absorption or total transmittance, whereas the absorption coefficient plot will always show the spectral structure no matter what absorber amount is specified.

The program which calculates single-frequency absorption is very similar with a few exceptions. The absorption coefficient is calculated for only one absorber at a time, however, calculations may be made for a number of absorber pressures and frequencies at the same time.

The other main difference is that the Lorentz line shape is not used, but rather a modification to the Lorentz line shape suggested by Trusty [6]. The alternate shape has the form

$$(12) \qquad k = \frac{C(\nu_m, n) S \alpha_L}{\pi\left[(\nu-\nu_0)^2+\alpha_L^2\right]} \qquad 0 \le |\nu - \nu_0| \le \nu_m$$

$$k = \frac{C(\nu_m, n) S \alpha_L}{\pi\left[\nu_m^2+\alpha_L^2\right]} \cdot \frac{\nu_m^n}{(\nu-\nu_0)^n} \qquad |\nu - \nu_0| \ge \nu_m ,$$

where

$$(13) \qquad C(\nu_m, n) = \frac{S}{2\left[\int_0^{\nu_m} k d\nu + \int_{\nu_m}^{\infty} k d\nu\right]}$$

is added so that the line strength has the usual definition of the integrated absorption coefficient over the entire line. The integrations in Equation (13) may be performed directly to give for $C(\nu_m, n)$

$$(14) \qquad C(\nu_m, n) = \frac{\pi}{2\left[\tan^{-1}(\nu_m) + \nu_m/((\nu_m^2 + 1)(n - 1))\right]}$$

The modification location ν_m and modifier power n are specified by the user. For $\nu_m \geq 30\ \alpha_L$ and $n = 2$, the modified shape reduces to the Lorentz shape. For $n < 2$ the alternate line shape has more wing absorption than the Lorentz shape and for $n > 2$ the wing absorption is less.

VI. CO_2 LASER MEASUREMENTS

A. Background

Measurements have recently been made of the absorption by water vapor of two CO_2 laser lines, R20 at 975.930 cm^{-1} and P20 at 944.194 cm^{-1}.

McCoy originally measured the water vapor absorption of the P20 line in 1968 [10]. It was, however, considered important to repeat the measurements since more sophisticated equipment is now available and precise knowledge of the air broadened water vapor absorption coefficient in the 10 μm region is of substantial importance.

The laser used for these measurement was a Sylvania Model 948 which uses a grating at one end for line selection. The laser has been modified slightly with the addition of an inexpensive frequency stabilizer. For the P20 measurements, the frequency stability was not necessary but the amplitude stability which resulted was helpful in increasing the reliability of the measurements. For the R20 measurements, the frequency stability was essential since the transmittance is a rapidly varying function of frequency.

B. Measurements on P(20) Line

The first set of measurements described are for absorption of the P20 CO_2 laser line by pure water vapor. The new measurements are presented in Figure 6 along with the work of McCoy. The dashed line represents a least squares fit of the new data to an expression of the form $k = ap^2$. The derived expression is given in the figure along with the expression representing McCoy's data.

The scatter in the data is an indication of the repeatability of measurements of cell transmittance with water vapor in the cell. The scatter in measurements of evacuated cell transmittance is much less. The scatter could be due to inability to determine water vapor pressure accurately enough, temperature effects, or possibly water condensation on the White cell mirrors. Nevertheless, it is felt that the new measurements are probably more accurate than those of McCoy because of the more sophisticated experimental equipment available.

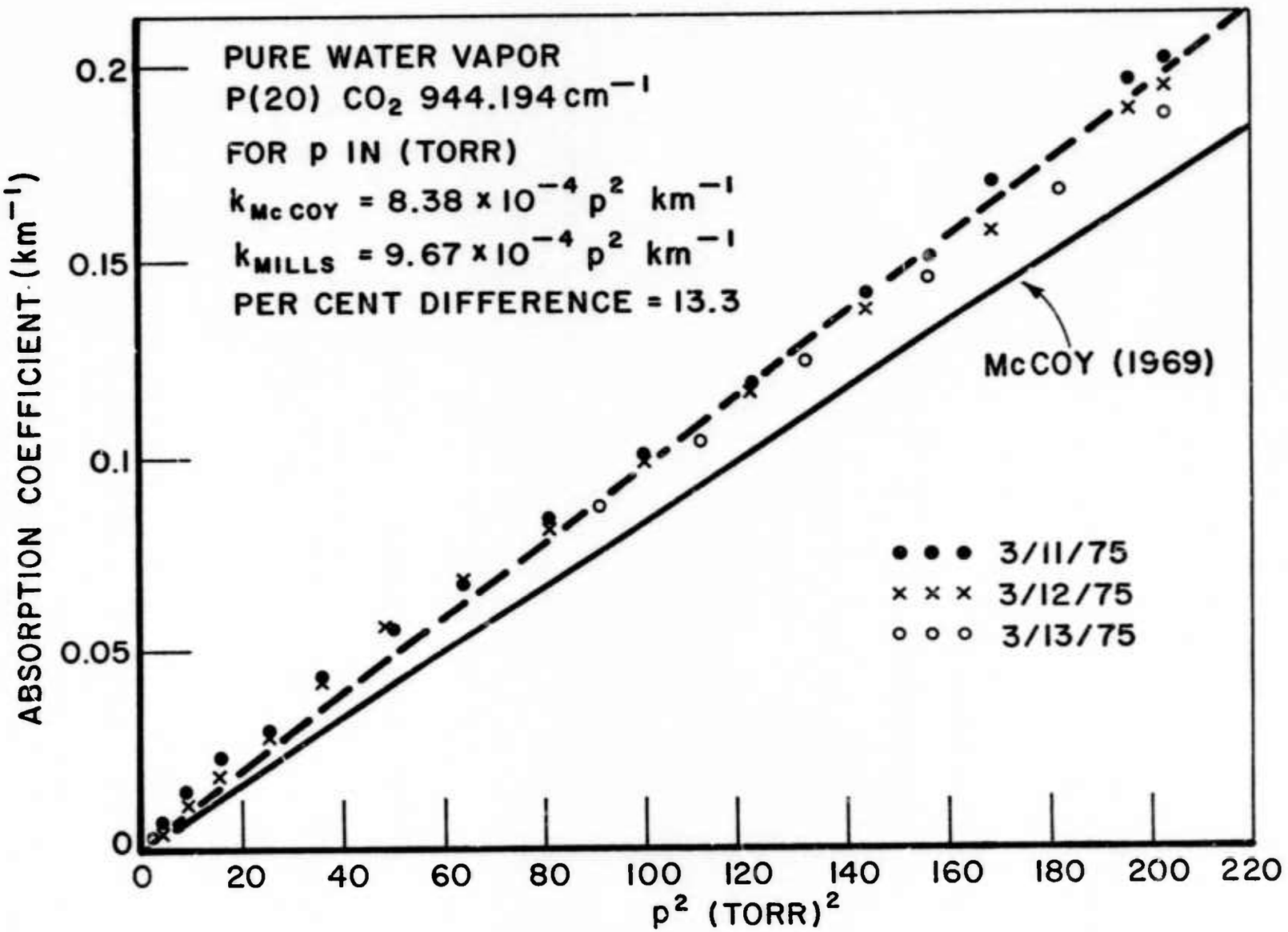

Fig. 6. Pure water vapor absorption at 944 19 cm^{-1}.

The next set of measurements are for absorption of the P20 line by water-vapor nitrogen mixtures at a total pressure of 760 torr. In 1968, McCoy made seven measurements at different water vapor pressures for air broadened samples. Analyzing this data in conjunction with his more extensive pure water vapor measurements he determined that the air broadened water vapor absorption could best be characterized for the P20 line by the following expression.

(15) $$k = 4.32 \times 10^{-6}\ p\ (P + 193p)\ km^{-1}$$

Here p is the water vapor pressure and P is the total pressure, both expressed in torr.

The most recent data were taken with a water vapor pressure of 14.27 torr and total pressure 760 torr. We also took some data in 1974 at water vapor pressures ranging from 14 to 15.1 torr. This data for 1974 and 1975 is presented in Table VIII with the 1974 values scaled to 14.27 torr using the expression derived by McCoy. These most recent results have all been averaged together resulting in an absorption coefficient of 0.23 km^{-1}. McCoy's expression gives .217 km^{-1} when evaluated at 14.27 torr.

TABLE VIII

WATER VAPOR-NITROGEN ABSORPTION FOR THE P20 CO_2 LASER LINE AT 944.194 cm^{-1}

Temperature is 23C to 25C; total pressure 760 torr.

Date	P H_2O (torr)	k (km^{-1})	k' (km^{-1}) (at 14.27 torr)
4/5/74	14	0.216	0.223
8/16/74	14.27	0.231	0.231
10/24/74	15.1	0.247	0.223
11/6/74	15	0.240	0.220
3/75	14.27	0.235	0.235
		0.216	0.216
		0.246	0.246
		0.260	0.260
		0.250	0.250
		0.213	0.213
		0.217	0.217
		Average	0.230

All the measurements in Table VIII have been made using a cell whose temperature is determined by room temperature which varied from 23C to 25C. These temperature variations may account for some of the data scatter.

Difficulties are encountered when attempting to describe the absorption by water vapor at 10.6 microns in terms of a simple theoretical model.

A consideration of the Lorentz line shape far from line center leads to the following expression for the absorption coefficient k in km^{-1}.

$$k = CpPe = Cp\,(P + (B - 1)\,p) \tag{16}$$

Here C is a constant, p is the partial pressure, P is the total pressure, and Pe is the effective pressure.

The approach McCoy used to obtain Equation (15) was the following. For pure water vapor, Equation (16) may be written

$$k = CBp^2 = C_1 p^2. \tag{17}$$

McCoy then found C_1 from his extensive pure water vapor data. Substituting C_1 from Eq. (17) into Eq. (16) gives

$$k = \frac{C_1}{B}\,p\,(P_b + Bp) \tag{18}$$

where C has been replaced by $\frac{C_1}{B}$ and P_b is the broadener pressure. He then used one of his air-broadened data points which he believed to be quite accurate, substituted for k in Eq. (18) and solved for B.

$$k_{exp.} = \frac{C_1}{B}\,p\,(P_b + Bp) \tag{19}$$

or

$$B = \frac{C_1\,p\,P_b}{k_{exp.} - C_1 p^2} \tag{20}$$

Using this procedure he obtained a value of !94 for B. Using the same procedure and the 1975 data, a value of 310 is obtained for B.

In Equation (2) the denominator is obtained by subtracting two numbers which are not very different. For instance, using the 1975 data

$k_{exp.}$ is .230 and C_1p^2 is .197. Therefore, a small percentage error in either $k_{exp.}$ or C_1p^2 would result in a much larger percentage error in $k_{exp.} - C_1p^2$ and therefore a large error in B.

Another method of determining B is to curve fit a number of air-broadened measurements at different partial pressures to an equation of the form $A_p + B_p^2$ and then rearrange the result in the desired form. Using this method with the seven points measured by McCoy in 1968 results in a value of 78 for B. The equations derived by either method fit the data equally well so it would appear that the value of B is quite uncertain.

A third method for determining B would be to use the classical Burch method, i.e., measure the transmittance of two samples having the same water content but different partial pressures using adjustment of the total pressure to cause equal transmittance of the two samples. Within the available limits of path length, total pressure, and water pressure (for a room temperature cell), the prospects for accurate results are not encouraging. That is, the transmittance just does not change much with increasing broadener pressure.

The whole idea of expressing the air broadened water vapor absorption at 10.6 μm in terms of B may be somewhat misleading, since it implies that the self-broadened half-width of the water line contributing to the absorption is anywhere from 80 to 300 times the foreign-broadened half-width. Investigations have been made of water lines in this region which show that this is clearly not true. It might be more appropriate to use a W or wing-lifting coefficient to describe the absorption. Meredith [12] has suggested that it would be better to express the absorption as follows.

$$k = C_s p^2 + C_f p P_f \tag{21}$$

and make no attempt to relate C_s and C_f since they may be caused by completely different mechanisms.

C. Measurements on the R20 Line

Measurements have been made of the absorption of the R20 CO_2 laser line at 975.930 cm^{-1} by water-vapor nitrogen mixtures at 760 torr total pressure. The results of the measurements are shown in Figure 7. The data points represent distinct measurements made over a period of several months. The line in the figure is the result of a least squares fit of the data to a straight line.

The fact that the data fit a straight line is an indication that the laser line is very close to a water vapor line. An examination of a calculated spectrum in the region of the laser line does indeed show a near coincidence of the laser line with an absorption line. In this situation

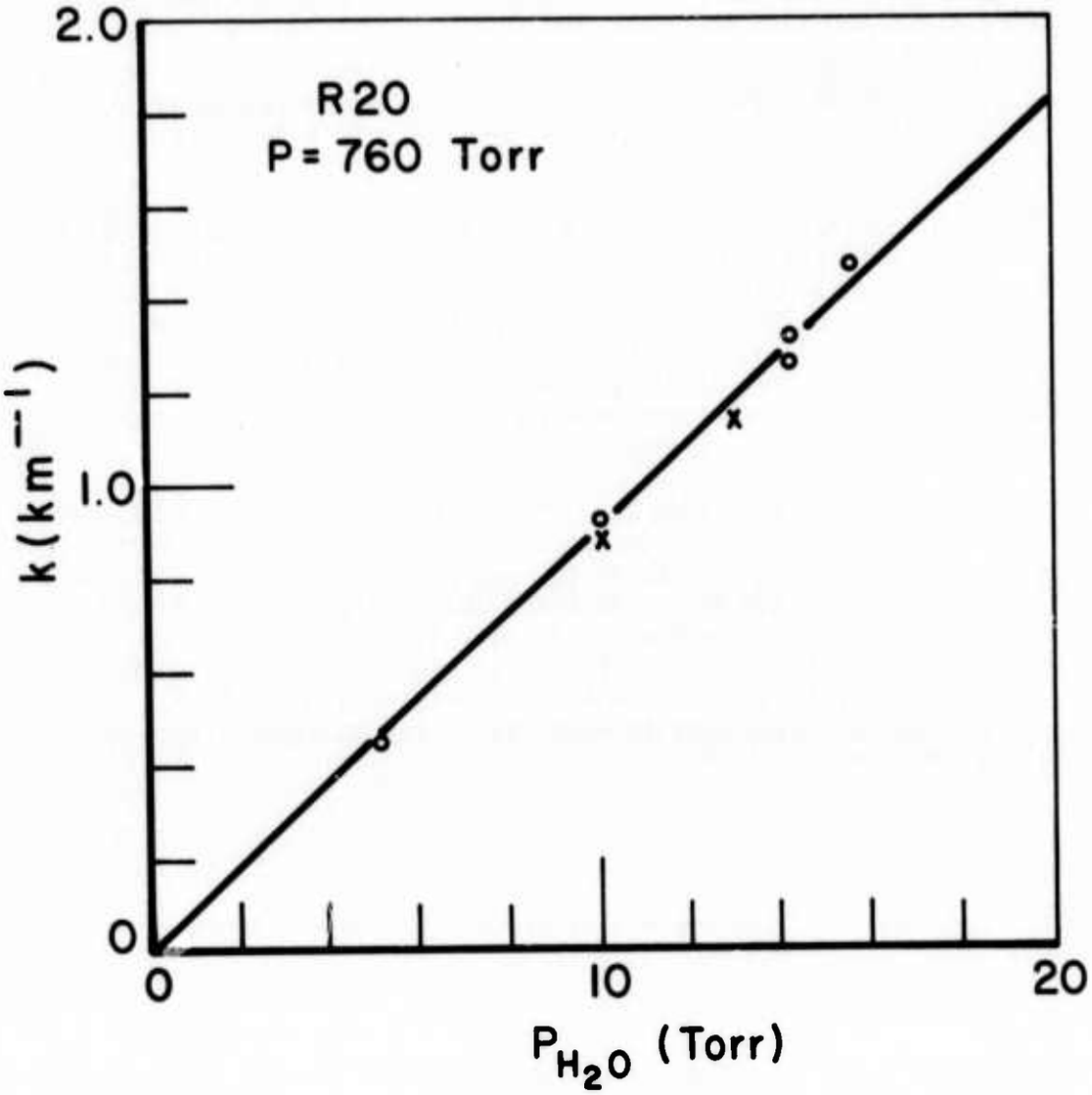

Fig. 7. Absorption of water vapor at 975.930 cm^{-1}.

it is possible to use techniques of laser spectroscopy to obtain information about the absorption line by measuring the absorption coefficient as a function of total pressure with the absorber pressure constant.

This can be shown by the following [1, 13]. For an isolated Lorentz line with fixed partial pressure, we have

$$k = \frac{S}{\pi} \frac{\alpha}{(\Delta\nu)^2 + \alpha^2} \tag{22}$$

where k is the absorption coefficient,

$$\alpha = \alpha_o \frac{Pe}{Po} \left(\frac{To}{T}\right)^m$$

is the half width of the absorption line, Po = 1 atm., $\Delta\nu$ is the difference in the frequencies of the absorption line and the laser line, Pe is the effective pressure and S is the line strength. For a constant temperature and P in atmospheres, α becomes $\alpha = \alpha_o Pe$.

On a curve of k versus effective pressure Pe, the condition for zero slope with $\Delta\nu$ constant is

$$\frac{dk}{d\alpha} = \left[\frac{S}{\pi} \frac{(\Delta\nu)^2 + \alpha^2 - 2\alpha^2}{((\Delta\nu)^2 + \alpha^2)^2}\right] = 0 \tag{23}$$

or,

$$\alpha = \Delta\nu \tag{24}$$

Therefore, as a first approximation (i.e., assuming a single isolated Lorentz line), the following expression holds:

$$\alpha_o Pe = \Delta\nu \tag{25}$$

Substituting back into the equation for k gives S, since at the zero slope condition

$$(26) \qquad k = \frac{S}{\pi} \frac{\Delta\nu}{\Delta\nu^2 + \Delta\nu^2}$$

$$= \frac{S}{2\pi\Delta\nu}$$

or

$$(27) \qquad S = 2\pi\Delta\nu k$$

where $k = -\frac{1}{u} \ln T$, and u is the absorber amount in molecules/cm^2.

Thus, if the frequency difference between the laser line and absorption line is accurately known, the half-width and strength can be accurately determined. In this case, the laser line frequency is well known, however, unfortunately neither the half-width nor the frequency of the absorption line is well known.

All is not lost, however. If the laser frequency can be tuned it should be possible to determine the half-width by making measurements at two different laser frequencies providing the laser frequency is close enough to the absorption line. Fortunately the frequency stabilizer used with our laser is capable of tuning the laser frquency to any point in the laser gain profile and maintaining it; and the laser line and absorption line are close enough together. This has not yet been done, but it will be shortly.

It is also possible to determine the self-broadening coefficient B using this procedure. The absorption coefficient is measured as a function of total pressure for two different absorber pressures. From Equation (25) we see that at zero slope the effective pressure for the measurement at absorber pressure p_1 must be the same as the effective pressure at zero slope for the measurement at absorber pressure p_2. Thus, we have

$$(28) \qquad P_{e1} = P_{e2}$$

or

$$(29) \qquad P_1 + (B - 1)p_1 = P_2 + (B - 1)p_2$$

where P_1 and P_2 are the total pressures at zero slope for measurement 1

and measurement 2, respectively. Solving Equation (29) for B we have

$$B = \frac{P_2 - P_1}{P_1 - P_2} + 1 \qquad (30)$$

The above experiment was performed using the R20 CO_2 laser line and partial pressures of water vapor of 3 torr and 10 torr. The results are shown in Figures 8 and 9, respectively. For the experiment at 3 torr the zero slope point is at P = 144 ±3 torr. For the 10 torr experiment the zero slope point is at P = 111 ±2 torr. Using these values and Equation (3), we obtain for B a value of 5.7 ±0.7.

VII. SPECTROPHONE CALIBRATION TECHNIQUES

The purpose of the spectrophone calibration experiment is to determine the most accurate and efficient method by which a spectrophone can be calibrated.

For absorption coefficient measurements, the spectrophone offers the advantage of increased sensitivity over the White cell but the disadvantage of requiring indirect calibration. The spectrophone's output (pressure) signal is directly proportional to the absorption coefficient; on the other hand, the White cell basic measurement corresponds directly to transmittance, from which the absorption coefficient is calculated. In the case of high transmittance, White cell measurements require taking the ratio of two nearly equal numbers. As was shown by Trusty [15], significant erros in the absorption coefficient can occur for a small error in the transmittance.

At the present time one of the principal problems in the use of the spectrophone is that for most accuracy it is necessary to use an indirect calibration from known White cell transmittances. Experience has also shown that the spectrophone must be independently calibrated for each laser line to be considered. Thus, each spectrophone experiment requires that accurate absorption data be known for the laser line being measured.

This investigation is intended to explore two other methods of spectrophone calibration, both of which are direct techniques.

The first method to be considered is based on the thermodynamic relationship between the absorption coefficient and the pressure rise in a laser irradiated spectrophone. For a CW laser as a source, it can be shown [15] that:

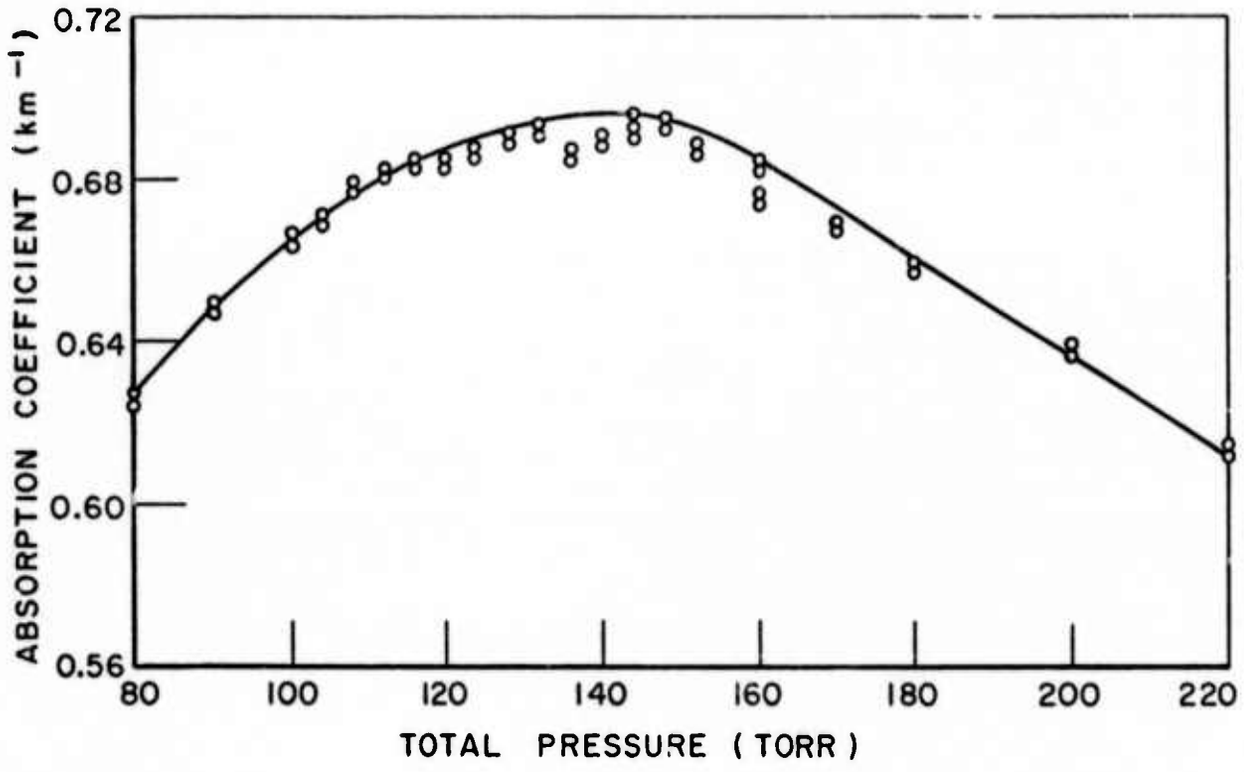

Fig. 8. Absorption at 975.930 cm^{-1} for 3 torr H_2O vs total pressure.

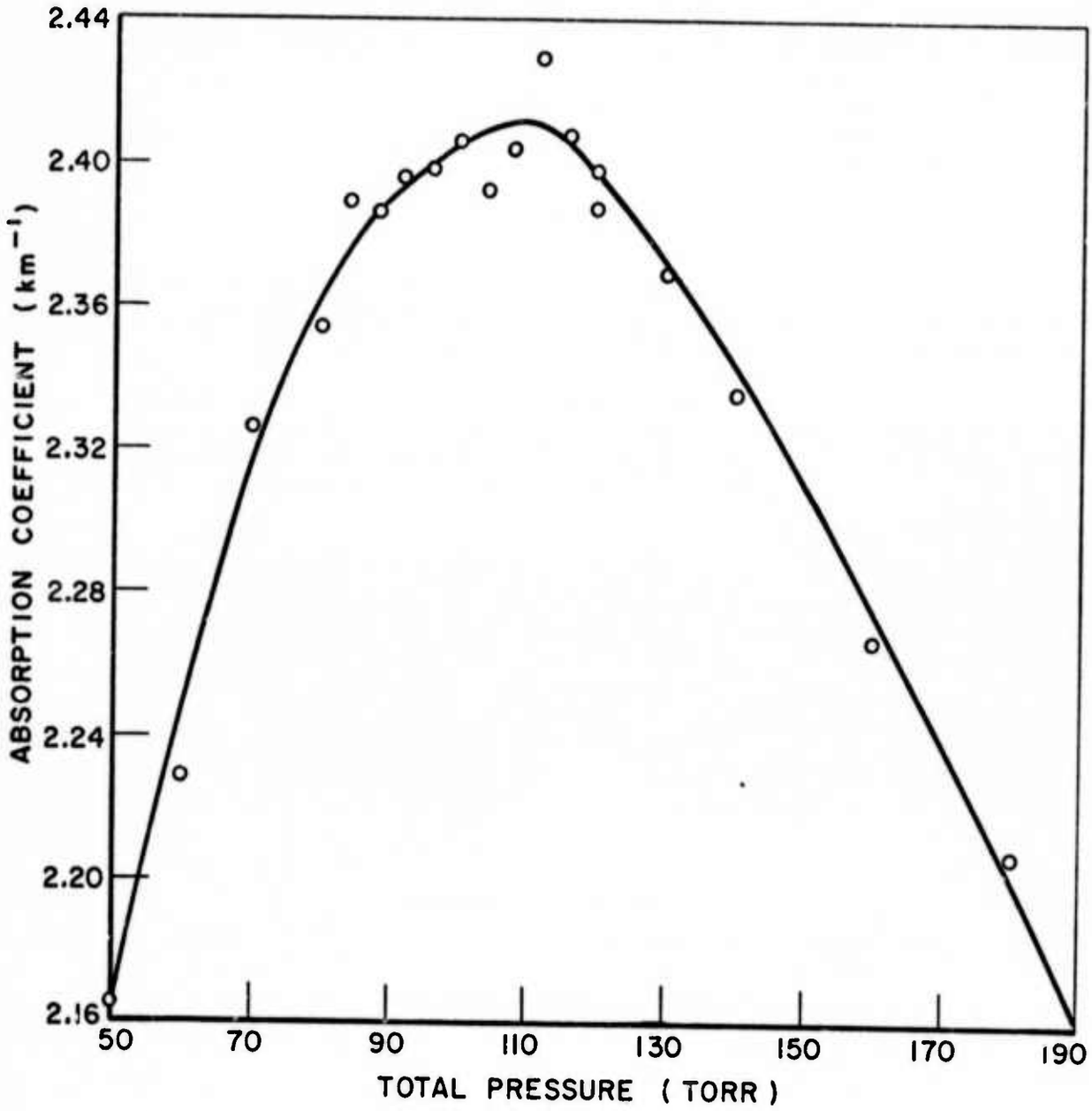

Fig. 9. Absorption at 975.930 cm^{-1} for 10 torr H_2O vs total pressure.

(31) $$\alpha = \frac{4\pi k \bar{T}}{WPB} p$$

where α = absorption/length
k = thermal diffusivity
T = ambient absolute temperature
W = total beam power
P = nominal pressure
B = geometric constant
p = pressure rise from nominal

Thus, given the thermodynamic properties of the gas sample and the laser intensity, it should be possible to calculate the absorption having measured the pressure rise.

The most serious difficulty encountered in this method is the accurate determination of the constant B. This requires knowledge of the laser spot size in the spectrophone cell. Any error in the determination of the spot size will have a large effect on the calculation of B (and thus α).

The second method to be considered requires irradiating a known gas sample confined within the spectrophone and measuring the initial pressure rise. The theory, then predicts that the initial slope of the pressure rise (as a function of time) is directly related to the absorption coefficient of the enclosed gas. The defining expression has been shown [16] to be

(32) $$\alpha = \frac{\Delta P_{max}\, 4\pi k}{(\gamma - 1) P_o \rho C_p}$$

where ΔP_{max} = maximum change in cell pressure
k = thermal conductivity
ρ = density of the gas
C_p = specific heat at constant pressure
P_o = laser power
γ = specific heat ratio

ΔP_{max} occurs at $t_{max} \leq \frac{D^2 \rho C_p}{16 k}$

where D = spectrophone diameter
t_{max} = time at which heat loss to the cell walls begins

This method requires that the pressure signal be accurately measured in the time interval $t_o \leq t \leq t_{max}$, where t_o is the time required for Δp to be uniformly distributed throughout the entire cell. This method eliminates the problem of determining the laser spot size since it based only upon the change in pressure, laser power, and the thermodynamic properties of the sample gas in the spectrophone.

The experiments which are now underway will compare the above two direct methods and the White cell comparison method. A 10 μm CO_2 laser will be used. The spectrophone will be the differential model which was described in a previous report [17]. For these experiments, an on-line digital computer will be used to facilitate data recording and analysis. The program evaluates the pressure signal or its slope as required and also utilizes averaging and smoothing routines to reduce uncertainties.

At the present time the experimental equipment has been completed but results have not been obtained.

VIII. DIODE LASER SPECTROSCOPY

Measurements of line strength, half-width, foreign broadening coefficients, and transmittance have been made using a 1945-1980 cm^{-1} $PbS_{1-x}Se_x$ diode. Individual laser modes scan an interval of about 0.8 cm^{-1}. Pressures from 0.1 to 760 torr have been used.

CO_2 absorption has been studied for J = 24 to 48 of the R branch of the 11'0-00°0 band.

N_2O absorption has been observed for J = 12 to 27 of the P branch of the 20°0-01'0 band. In addition, the Q branch of this band has been studied.

Both pure and foreign broadening has been studied. Broadening gases were nitrogen and helium.

These results are being analyzed to produce tables of line strength and half-width and will be described in detail in an upcoming technical report.

In addition, measurements of water vapor absorption were made using the laser diode to simulate the 6-5 P(10) [1973.299 cm^{-1}] and 6-5 P(14) [1957.050 cm^{-1}] lines of the CO laser. Good agreement with previous results was obtained.

IX. DESIGN OF CO, CO_2, AND DF PROBE LASER

The general experimental program requires stable lasers of low and moderate power which will operate at any of the wavelengths of interest. In some cases, a gas dynamic or chemical laser operates on spectral lines which cannot be obtained with an electrically excited laser (e.g., CO).

The CO probe laser [18] previously used on this program was a cooled, sealed off system with a grating for single line operation. With a sealed off system, unexcited CO molecules exist between the electrodes and mirrors, and prevent laser operation at the lower vibrational levels. Since these levels have become of greater interest, a flowing system patterned after that of Djeu [19] with a one meter, liquid nitrogen cooled, active length and 1.5 meter grating-tuned optical cavity is being constructed. This system was very briefly operational before mechanical failure of the laser tube. This port of the laser has been redesigned with glass bellows and the new tube is now being mounted, and several other minor design modifications are being made. It is expected to be operational shortly. The main benefit of the flowing system is the opportunity to use a continuous helium flush in the inactive region between the windows and electrodes, thus allowing operation at levels as low as the 1-0 band.

A one meter grating-tuned CO_2 laser is also under construction. It has a small bore water cooled active length, and employs an active stabilization [20] circuit to control the PZT length control to maintain operation at line center. Stable single line operation at several watts is expected.

A one watt DF laser, following the design of Hinchen [21], is being developed. This system uses a dc discharge in an SF_6 mixture to furnish free fluorine, with the deuterium being injected in a subsonic flow channel downstream. Hinchen's system operated very well on HF, but its gain was marginal for DF excitation. Consequently, for the OSU laser the active length is being doubled by using two, four-inch channels in the laser cavity. This will allow one channel to be cut off, with subsequent savings in fuel costs, when the extra gain is not required. All major components are now on hand, including the dc power supply, electroformed channels, and optics. Mechanical construction is proceeding.

X. REFERENCES

1. F.S. Mills and R.K. Long, "Measured N_2O-N_2 Absorption at Five DF Laser Frequencies," Report 3271-9, March 1974, The Ohio State University ElectroScience Laboratory, Department of Electrical Engineering; prepared under contract F30602-72-C-0016 for Rome Air Development Center. (RADC-TR-74-89) (AD 778 949)

2. F.S. Mills and R.K. Long, "Absorption Coefficient Measurements of CO_2, HDO-N_2, and CH_4-Air Using a DF Laser," Report 3271-10, August 1974, The Ohio State University ElectroScience Laboratory, Department of Electrical Engineering; prepared under contract F30602-72-C-0016 for Rome Air Development Center. (RADC-TR-74-295) (AD A001097)

3. R.K. Long, F.S. Mills, and G.L. Trusty, "Calculated Absorption Coefficients for DF Laser Frequencies," Report 3271-7, November 1973, The Ohio State University ElectroScience Laboratory, Department of Electrical Engineering; prepared under contract F30602-72-C-0016 for Rome Air Development Center. (RADC-TR-74-95) (AD 775373)

4. E.K. Damon, J.C. Peterson, F.S. Mills, and R.K. Long, "Spectrophone Measurement of the Water Vapor Continuum at DF Laser Frequencies," Report 4054-1, July 1975, The Ohio State University ElectroScience Laboratory, Department of Electrical Engineering; prepared under contract F30602-75-C-0029 for Rome Air Development Center.

5. C.J. Ultee, The Review of Scientific Instruments, 42, (1971), p. 1174-1176.

6. R.K. Long, F.S. Mills, and G.L. Trusty, "Experimental Absorption Coefficients for Eleven CO Laser Lines," Report 3271-5, March 1973, The Ohio State University ElectroScience Laboratory, Department of Electrical Engineering; prepared under contract F30602-72-C-0016 for Rome Air Development Center. (RADC-TR-73-126) (AD 760140)

7. R.K. Long, "Laser Absorption in the 5 Micron Band," Report 3271-1, November 1971, The Ohio State University ElectroScience Laboratory, Department of Electrical Engineering; prepared under contract F30602-72-C-0016 for Rome Air Development Center. (RADC-TR-71-314) (AD 736037)

8. R.A. McClatchey, et al., AFCRL-TR-73-0096, January 1973.

9. E.M. Deutschman and R.F. Calfee, "Two Computer Programs to Produce Theoretical Absorption Spectra of Water Vapor and Carbon Dioxide," (AD 816 369), April 1967.

10. J.H. McCoy, D.B. Rensch, and R.K. Long, Applied Optics 8, 1471, (1969)

11. D.E. Burch, E.B. Singleton, D. Williams, Applied Optics 1, 359, (1962)

12. R.E. Meredith, T.W. Tuer, D.R. Woods, "Investigation of DF Laser Propagation," Ecom-74-4, December 1974. (OSD-1366)

13. G.L. Trusty, "Laser Propagation Investigation," Final Report 2819-5, The Ohio State University ElectroScience Laboratory, Department of Electrical Engineering, Internal Final Report, January 1973.

14. W.S. Benedict and L.D. Kaplan, J. Chem. Physics, Vol. 30, 388 (1959).

15. G.L. Trusty, "Absorption Measurements of the 10.4 Micron Region Using a CO_2 Laser and a Spectrophone," Report 2819-4, January 1973, The Ohio State University ElectroScience Laboratory, Department of Electrical Engineering; prepared under contract F33615-69-C-1807 for Air Force Avionics Laboratory, Wright-Paterson Air Force Base. (AFAL-TR-72-413) (AD 907549)

16. F.G. Gebhardt (United Technology Corp. Research Laboratories), Private Communication.

17. E.K. Damon, et al., "Spectrophone Measurement of the Water Vapor Continuum at DF Laser Frequencies," Report 4054-1, July 1975, The Ohio State University ElectroScience Laboratory, Department of Electrical Engineering; prepared under contract F30602-75-0029 for Rome Air Development Center.

18. C. Freed, Applied Physics Letters, Vol. 18, p. 456-61, 15 May 1971.

19. N. Djeu, Appl. Phys. Letters, Vol. 23, No. 6, p. 309-10, 15 Sept 1973.

20. W.H. Thomason and D.C. Elbers, "An Inexpensive Method to Stabilize the Frequency of a CO_2 Laser," OSA Annual Meeting, Houston, Texas, 15 October 1974.

21. J. Hinchen, Private Communications.

22. D. Burch, D.A. Gryvnak, J. D. Pembrook, AFCRL-71-0124, Ford Aeronutronic Report U-4897, January 1971.

☆U.S. GOVERNMENT PRINTING OFFICE: 1975-614-357/52